



Published in final edited form as:

*Oncogene*. 2017 June 15; 36(24): 3477–3489. doi:10.1038/onc.2016.499.

## The miR-487b-3p/GRM3/TGF $\beta$ signaling axis is an important regulator of colon cancer tumorigenesis

Haowei Yi<sup>2</sup>, Liying Geng<sup>1</sup>, Adrian Black<sup>1</sup>, Geoff Talmon<sup>4</sup>, Lyudmyla Berim<sup>5</sup>, and Jing Wang<sup>1,2,3,\*</sup>

<sup>1</sup>Eppley Institute for Research in Cancer and Allied Diseases, University of Nebraska Medical Center, 985950 Nebraska Medical Center, Omaha, NE 68198, USA

<sup>2</sup>Department of Genetics, Cell Biology and Anatomy, University of Nebraska Medical Center, 985950 Nebraska Medical Center, Omaha, NE 68198, USA

<sup>3</sup>Department of Biochemistry and Molecular Biology, University of Nebraska Medical Center, 985950 Nebraska Medical Center, Omaha, NE 68198, USA

<sup>4</sup>Department of Pathology and Microbiology, University of Nebraska Medical Center, 985950 Nebraska Medical Center, Omaha, NE 68198, USA

<sup>5</sup>Department of Internal Medicine Oncology/Hematology, University of Nebraska Medical Center, 985950 Nebraska Medical Center, Omaha, NE 68198, USA

### Abstract

Molecular targeting is an important strategy to treat advanced colon cancer. The current study demonstrates that expression of GRM3, a metabotropic glutamate receptor mainly expressed in mammalian central nervous system, is significantly upregulated in majority of human colonic adenocarcinomas tested and colon cancer cell lines. Knockdown of GRM3 expression or inhibition of GRM3 activation in colon cancer cells reduces cell survival and anchorage-independent growth *in vitro* and inhibits tumor growth *in vivo*. Mechanistically, GRM3 antagonizes TGF $\beta$ -mediated activation of protein kinase A and inhibition of AKT. In addition, TGF $\beta$  signaling increases GRM3 protein stability and knockdown of GRM3 enhances TGF $\beta$ -mediated tumor suppressor function. Further studies indicate that miR-487b-3p directly targets GRM3. Overexpression of miR-487b-3p mimics the effects of GRM3 knockdown and suppresses the tumorigenicity of colon cancer cells *in vivo*. Expression of miR-487b-3p is decreased in colon adenocarcinomas and inversely correlates with GRM3 expression. Taken together, these studies indicate that upregulation of GRM3 expression is a functionally important molecular event in colon cancer, and that GRM3 is a promising molecular target for colon cancer treatment. This is particularly interesting and important from a therapeutic standpoint because numerous metabotropic glutamate receptor antagonists are available, many of which have been found unsuitable for treatment of

---

Users may view, print, copy, and download text and data-mine the content in such documents, for the purposes of academic research, subject always to the full Conditions of use:[http://www.nature.com/authors/editorial\\_policies/license.html#terms](http://www.nature.com/authors/editorial_policies/license.html#terms)

\*Corresponding Author: Jing Wang, University of Nebraska Medical Center, 985950 Nebraska Medical Center, Omaha, NE 68198, USA, Tel: 402-559-5558, Fax: 402-559-7319, [jjwang@unmc.edu](mailto:jjwang@unmc.edu).

### CONFLICT OF INTEREST

There are no competing financial interests in relation to the work described.

neuropsychiatric disorders for reasons such as inability to readily penetrate blood brain barriers. Since GRM3 is upregulated in colon cancer, but rarely expressed in normal peripheral tissues, targeting GRM3 with such agents would not likely cause adverse neurological or peripheral side effects, making GRM3 an attractive and specific molecular target for colon cancer treatment.

### Keywords

GRM3; TGF $\beta$ ; miR-487b-3p; colon cancer; PKA; AKT

## INTRODUCTION

Treatment of advanced colon cancer with molecularly targeted drugs has not had large clinical impact in part due to high degree of heterogeneity. Therefore, there is a need to identify new molecule targets and develop efficient target-specific therapies.

Glutamate functions as a major excitatory neurotransmitter in mammalian central nervous system (CNS) (1;2). Glutamate signaling is mediated by two classes of glutamate receptors, ionotropic and metabotropic receptors (3). Metabotropic receptors (mGluR), a group C family of G-protein-coupled receptors (GPCRs), consist of eight members, classified into three subtypes (4;5). Group I receptors (mGluR1 and 5) are coupled to phospholipase C leading to activation of protein kinase C, whereas group II (mGluR2 and 3) and group III (mGluR4, 6, 7 and 8) receptors are negatively coupled to adenylyl cyclase, inhibiting production of cyclic AMP (cAMP) (3–5). Although glutamatergic system is mainly restricted to the CNS, expression of functional glutamate receptors has been reported in non-neuronal peripheral cells such as skin and pancreatic islets (6;7). Furthermore, studies have revealed that glutamate signaling is dysregulated and may play a role in cancer (8–10).

GRM3 is the gene encoding mGluR3, which is frequently mutated in melanoma (11). Mutant GRM3 selectively activates MEK, leading to increased anchorage-independent growth and migration (11). Activation of GRM3 has been reported to suppress bone morphogenetic protein (BMP) signaling and sustain tumorigenic potential of glioma-initiating cells (12). Pharmacological blockade of GRM3 reduced growth of glioma cells *in vitro* and *in vivo* (13–15). These studies suggest that GRM3 plays a role in cancer and could be a potential target for cancer treatment.

Transforming growth factor  $\beta$  (TGF $\beta$ ) signaling plays a dual role in cancer. While studies show that TGF $\beta$  promotes metastasis and is associated with worse prognosis (16–19), others demonstrate that it suppresses tumorigenicity and metastasis (20–26) and that loss or reduction of TGF $\beta$  signaling is associated with development of metastasis (27;28). In genetically engineered mouse models, inactivation of TGF $\beta$  signaling increases malignancy and invasiveness of intestinal tumors of Apc mutant mice (29–33).

MicroRNAs (miRNAs) are a group of small non-protein coding RNAs evolutionarily conserved (34). MiRNAs suppress expression of gene targets at the posttranscriptional level through sequence-specific interaction with the 3'-untranslated regions (UTR), leading to

translation inhibition or mRNA degradation (35). Alterations in miRNA expression are found to be associated with many human cancers (36).

Here we demonstrate that GRM3 expression is significantly upregulated in majority of human colonic adenocarcinomas tested and colon cancer cell lines. Knockdown of GRM3 expression or pharmacological blockade of GRM3 in colon cancer cells reduces cell survival and anchorage-independent growth *in vitro* and inhibits tumor growth *in vivo*.

Mechanistically, GRM3 antagonizes TGF $\beta$ -mediated activation of protein kinase A (PKA) and inhibition of AKT activation. In addition, TGF $\beta$  signaling increases GRM3 protein stability and knockdown of GRM3 expression enhances TGF $\beta$ -mediated tumor suppressor function. Further studies indicate that GRM3 is a direct target of miR-487b-3p and that miR-487b-3p mimics the effects of GRM3 knockdown in colon cancer cells *in vitro* and *in vivo*. Expression of miR-487b-3p is decreased in colon adenocarcinomas and inversely correlates with GRM3 expression. Taken together, these studies indicate that the miR-487b-3p/GRM3/TGF $\beta$  signaling axis is an important regulator of colon cancer tumorigenesis and that upregulation of GRM3 is a functionally important molecular event in colon cancer. Therefore, GRM3 is a promising molecular target for colon cancer treatment. This is particularly interesting and important from a therapeutic standpoint because numerous metabotropic glutamate receptor antagonists are available (37), many of which have been found unsuitable for treatment of neuropsychiatric disorders due to their inability to readily penetrate blood brain barriers. Since GRM3 is upregulated in colon cancer, but rarely expressed in normal peripheral tissues, targeting GRM3 with such agents would not likely cause adverse neurological or peripheral side effects, making GRM3 an attractive and specific molecular target for colon cancer treatment.

## RESULTS

### Expression of GRM3 is markedly increased in colon cancer specimens

Although it has been implicated that GRM3 is an important player in melanoma and glioma (11–15), it is unknown whether GRM3 plays a role in colon cancer. GRM3 expression was therefore examined in human specimens using immunohistochemistry (IHC) analysis. Verification of the anti-GRM3 antibody is shown in Fig. 3c. Tissue micro-arrays (TMAs) consisting of 29 normal colon and 65 colon adenocarcinomas were analyzed. Mouse brain tissue was used as a positive control. GRM3 expression was very low in normal colon epithelium, but increased significantly in colon tumors (Fig. 1a). Quantification showed that the average intensity of GRM3 staining and percentage of GRM3 positive cells were approximately 5.5-fold and 3.8-fold higher respectively in tumors than in normal colon (Fig. 1b & 1c). In addition, GRM3 expression was increased in more than 90% of colon tumors examined (Fig. 1b & 1c). These results demonstrate that GRM3 expression is upregulated in majority of colon adenocarcinomas. However, analysis of TCGA databases revealed that GRM3 mRNA was not increased in colon adenocarcinomas (data not shown).

### GRM3 is critical for tumor growth *in vivo*

These observations prompted us to investigate whether GRM3 plays a functional role in colon cancer. A panel of human colon cancer cell lines and an immortalized human colon

epithelial cell line, HCEC (38), were used. HCT116 and RKO cells are defective in TGF $\beta$  signaling due to lack of TGF $\beta$  RII (39). HCT116b cells were isolated from the same colon tumor as HCT116, but displayed much lower metastatic potential (40). FET cells, isolated from a well differentiated colon tumor, are sensitive to TGF $\beta$ -mediated growth inhibition and apoptosis (20). CBS and GEO cells are partially responsive to TGF $\beta$  due to low TGF $\beta$  RII and RI expression, respectively (22;41). HT29 cells do not express Smad4 due to mutations (42). All cell lines bear either KRAS or BRAF mutations, and all except RKO (43) have mutated APC or  $\beta$ -catenin.

GRM3 expression was much higher in colon cancer cells than in HCECs (Fig. 2a, left), consistent with the results from human specimens. However, GRM3 mRNA levels were similar between HCECs and most of colon cancer cell lines (Fig. 2a, middle and right), suggesting that upregulation of GRM3 may be through post-transcriptional mechanism(s). Of note, expression of GRM2, the other member of group II metabotropic glutamate receptors, was almost undetectable in all cell lines (Fig. 2a, middle). Mouse brain tissue was used as a positive control. These results indicate that expression of GRM3 but not GRM2 is increased in colon cancer cells.

To determine GRM3 function, its expression was knocked down in FET, CBS and HCT116, three colon cancer cell lines with different genetic background. Each of two independent shRNAs (sh1 and sh2) reduced GRM3 expression by more than 90% as compared to a scrambled shRNA and had no effect on GRM2 expression (Fig. 2b, data not shown). Knockdown of GRM3 increased sensitivity to growth factor deprivation stress (GFDS)-induced apoptosis, reflected by enhanced PARP cleavage (Fig. 2c) and increased apoptosis in DNA fragmentation assays (Fig. 2d). In addition, GRM3 knockdown decreased anchorage-independent growth (Fig. 2e, Fig. S1a and S1b) and inhibited motility and migration (Fig. 2f).

We next examined the effect of GRM3 knockdown *in vivo*. Mice were subcutaneously injected with CBS cells stably expressing a scrambled shRNA or GRM3 shRNAs. Xenograft tumor growth curves showed that tumors of GRM3 shRNA-expressing cells (designated GRM3 shRNA tumors) grew at a significantly lower rate than those of control cells (designated control tumors) (Fig. 3a). As a result, GRM3 shRNA tumors were much smaller than control tumors (Fig. 3b). IHC staining confirmed GRM3 knockdown in GRM3 shRNA tumors and verified the specificity of the anti-GRM3 antibody (Fig. 3c). TUNEL and Ki67 staining showed much more apoptotic cells and fewer proliferative cells in GRM3 shRNA tumors than in control tumors (Fig. 3d). These results indicate that knockdown of GRM3 inhibits tumor growth *in vivo* and that this inhibitory effect is a combined result of increased apoptosis and suppressed proliferation.

### A GRM3 antagonist mimics GRM3 knockdown *in vitro* and *in vivo*

LY341495 is a potent and selective antagonist of GRM2/3 (44). As shown in Fig. 4a and Fig. S1c, LY341495 reduced colony formation of HCT116 cells in soft agar. When mice subcutaneously injected with HCT116 cells were treated with LY341495, tumors grew at a slower rate than those treated with vehicle control (Fig. 4b). Therefore, tumors were markedly smaller in LY341495-treated group than in control group (Fig. 4c). TUNEL and

Ki67 staining showed that LY341495 increased apoptotic cells and decreased proliferative cells (Fig. 4d). These results indicate that pharmacological blockade of GRM3 reduces anchorage-independent growth *in vitro* and tumor growth *in vivo*.

### GRM3 antagonizes TGF $\beta$ to regulate cell survival through the PKA/AKT signaling axis

GRM3 is negatively coupled to adenylyl cyclase, inhibiting production of cAMP (3–5). Since cAMP activates PKA (45), which inhibits AKT activation (23), activation of PKA and AKT was determined. PKA activity assays showed that knockdown of GRM3 increased PKA activity (Fig. 5a). Phosphorylation of CREB, a target of PKA (45), was also used to indicate PKA activity. Knockdown of GRM3 increased pCREB and decreased pAKT (Fig. 5b, left and Fig. 5c). Treatment with LY341495 or forskolin, a PKA activator, showed similar effect (Fig. 5b, middle). Complementarily, overexpression of GRM3 reduced pCREB and increased pAKT (Fig. 5b, right). These results indicate that GRM3 inhibits PKA and activates AKT in colon cancer cells.

To determine whether PKA is involved in GRM3-mediated cell survival, the PKA catalytic  $\alpha$  subunit (PKAC $\alpha$ ) was knocked down in FET cells (46). GRM3 knockdown-induced PKA activation and AKT inhibition were abrogated (Fig. 5d, right). Consequently, knockdown of PKAC $\alpha$  attenuated GRM3 knockdown-mediated increase of apoptosis under GFDS (Fig. 5e). These results indicate that GRM3 knockdown inhibits AKT and suppresses cell survival through PKA activation.

Unlike GRM3's coupling to cAMP (3–5), TGF $\beta$  activates PKA independent of cAMP, which inhibits AKT and suppresses cell survival (23). We confirmed TGF $\beta$  effect on pCREB and pAKT in FET cells (Fig. 5d, left). Since GRM3 knockdown and TGF $\beta$  activate PKA independently, we determined whether combination of both would further activate PKA and inhibit AKT. The results showed that GRM3 knockdown and TGF $\beta$  treatment concomitantly led to additional increase in pCREB and decrease in pAKT (Fig. 5d, left). As a result, when cells were treated with TGF $\beta$  under GFDS for 14 hours, TGF $\beta$  had little effect in control cells but induced apoptosis in GRM3 knockdown cells (Fig. 5f). In addition, GRM3 knockdown sensitized FET cells to TGF $\beta$ -mediated inhibition of anchorage-independent growth (Fig. 5g and Fig. S1a). These results indicate that GRM3 antagonizes TGF $\beta$ -mediated tumor suppressor function and that GRM3 knockdown enhances TGF $\beta$  effects.

To determine the mechanism underlying collaborative effect of TGF $\beta$  and GRM3 knockdown on PKA/AKT activation, cell survival and anchorage-independent growth, we investigated whether GRM3 mediates TGF $\beta$  signaling and found that GRM3 knockdown had no effect on expression of Smad2, Smad3, Smad4 or on canonical TGF $\beta$  signaling (data not shown). However, TGF $\beta$  increased GRM protein expression in FET and CBS cells (Fig. 5h, left and middle) while had little effect on GRM3 mRNA (Fig. 5i). Inactivation of TGF $\beta$  signaling by a dominant negative TGF $\beta$  RII (DNRII) in FET cells (20;41) abrogated TGF $\beta$  effect on GRM3 expression (Fig. 5h, right). Time course experiments showed that TGF $\beta$  increased GRM3 expression as early as 30 minutes (Fig. 5j), suggesting that TGF $\beta$  may increase GRM3 protein stability. Treatment with cycloheximide indicated that TGF $\beta$  markedly increased the half-life of GRM3 protein (Fig. 5k). Moreover, knockdown of

Smad2 or Smad3 attenuated TGF $\beta$ -induced GRM3 protein expression but had little effect on GRM3 mRNA levels (Fig. 5l), indicating that Smad2/3 contributes to TGF $\beta$ -mediated GRM3 protein expression.

### **MiR-487b-3p regulates GRM3 expression in colon cancer cells**

Although TGF $\beta$  increases GRM3 expression (Fig. 5h), it cannot fully explain ubiquitous upregulation of GRM3 expression in colon cancer cell lines regardless of their response to TGF $\beta$  signaling (Fig. 2a, left). Since GRM3 expression may be regulated post-transcriptionally (Fig. 2a), we turned our attention to miRNAs, which function as post-transcriptional regulators of mRNA expression and/or translation (35). We performed an *in silico* search for putative miRNA-binding sites in the 3'UTR of human GRM3 mRNA using TargetScan (47), PicTar (48) and miRanda-mirSVR (49). Among miRNA candidates conserved between human and mouse, miR-487b-3p was identified as a potential regulator of GRM3. Q-PCR assays indicated that expression of miR-487b-3p was much lower in colon cancer cell lines than in HCECs (Fig. 6a), suggesting that decreased miR-487b-3p expression may contribute to upregulated GRM3 expression in colon cancer cells.

To demonstrate that miR-487b-3p regulates GRM3 expression, miR-487b precursor was stably infected into FET and CBS cells. As a result, expression of mature miR-487b-3p was significantly increased (Fig. 6b, left). Complementarily, a chemically synthesized miR-487b-3p inhibitor markedly reduced endogenous miR-487b-3p expression (Fig. 6b, right). Overexpression of miR-487b-3p decreased GRM3 protein expression whereas the inhibitor increased GRM3 protein expression (Fig. 6c, left). However, GRM3 mRNA expression was not affected (Fig. 6c, right). These results indicate that miR-487b-3p suppresses GRM3 expression by inhibiting its translation. To determine whether GRM3 is a direct target of miR-487b-3p, 3'-UTRs of GRM3 containing potential miR-487b-3p recognition element or mutated seed sequence (Fig. 6d, left) was cloned into a luciferase construct. Luciferase assays revealed that miR-487b-3p repressed wild type but not mutant 3'-UTRs of GRM3 (Fig. 6d, right). These results indicate that GRM3 is a direct target of miR-487b-3p. Of note, miR-487b-5p did not target GRM3 (Fig. S2).

### **MiR-487b-3p regulates PKA/AKT activation and mimics GRM3 knockdown effect in colon cancer cells**

Similar to GRM3 knockdown, miR-487b-3p enhanced PKA activity (Fig. 6e), increased pCREB and decreased pAKT (Fig. 6f). MiR-487b-3p-expressing cells displayed increased apoptosis under GFDS (Fig. 6g) and decreased anchorage-independent growth (Fig. 6h and Fig. S3), indicating that miR-487b-3p mimicked the effect of GRM3 knockdown. In contrast, the miR-487b-3p inhibitor decreased GFDS-induced apoptosis (Fig. 6i).

To determine whether miR-487b-3p-mediated effect could be reversed by restoration of GRM3 expression, GRM3 cDNA was infected into miR-487b-3p-expressing cells (Fig. 6j). Ectopically expressed GRM3 is resistant to miR-487b-3p inhibition due to the lack of 3'-UTR. Restored GRM3 expression reversed miR-487b-3p-mediated increase of apoptosis (Fig. 6k). These results indicate that miR-487b-3p sensitizes colon cancer cells to GFDS-induced apoptosis through down-regulation of GRM3.

To demonstrate that miR-487b-3p enhances TGF $\beta$ -mediated tumor suppressor function, FET cells were treated with TGF $\beta$  under GFDS for 14 hours. TGF $\beta$  induced apoptosis in miR-487b-3p-expressing cells but not in control cells (Fig. 7a). In addition, TGF $\beta$  inhibited anchorage-independent growth by 96% in miR-487b-3p-expressing cells but only by 50% in control cells (Fig. 7b and Fig. S3a). Restoration of GRM3 expression reversed miR-487b-3p-mediated sensitization to TGF $\beta$ -induced apoptosis (Fig. 7c). Complementarily, FET cells were treated with TGF $\beta$  under GFDS for 24 hours. While TGF $\beta$  induced apoptosis in control cells, the miR-487b-3p inhibitor attenuated TGF $\beta$ -induced apoptosis (Fig. 7d). These results indicated that miR-487b-3p enhances TGF $\beta$ -induced apoptosis by repressing GRM3 expression and that inhibition of miR-487b-3p antagonizes TGF $\beta$  effect. Of note, TGF $\beta$  does not regulate miR-487b-3p expression (data not shown).

### MiR-487b-3p inhibits tumor growth in vivo

To determine the function of miR-487b-3p *in vivo*, athymic nude mice were subcutaneously inoculated with CBS control or miR-487b-3p-expressing cells. Xenograft tumor growth curves indicated that tumors of control cells (designated control tumors) grew at a significantly higher rate than those of miR-487b-3p-expressing cells (designated miR-487b-3p tumors) (Fig. 8a). Consequently, control tumors were much bigger than miR-487b-3p tumors (Fig. 8b). Analysis of GRM3 expression showed that the intensity of GRM3 staining and percentage of GRM3 positive cells were notably lower in miR-487b-3p tumors than in control tumors (Fig. 8c). Moreover, TUNEL and Ki67 staining indicated more apoptotic cells and fewer proliferative cells in miR-487b-3p tumors than in control tumors (Figs. 8d & 8e). These results demonstrate that miR-487b-3p suppresses GRM3 expression and inhibit tumor growth *in vivo*.

### Expression of miR-487b-3p is decreased in colon cancer specimens

To explore clinical relevance of miR-487b-3p, its expression was determined by *in situ* hybridization in the same sets of TMAs utilized in Figure 1. The staining intensity of miR-487b-3p was much stronger in miR-487b-3p-expressing tumors than in control tumors (Fig. 9a), verifying the specificity of the probe. Analysis of TMAs indicated that miR-487b-3p expression was very high in normal colon epithelium, but decreased markedly in colon tumors (Fig. 9b). Quantification of staining showed that the average intensity was significantly lower in colon adenocarcinomas than in normal colon (Fig. 9c), which is consistent with results from TCGA databases (Fig. S4). In addition, the correlation study revealed a significant inverse correlation between miR-487b-3p and GRM3 expression (Fig. 9d, \*\*\*  $P = 0.0003$ ). These results demonstrate that miR-487b-3p expression is decreased in colon adenocarcinomas and that miR-487b-3p expression is inversely correlated with GRM3 expression.

Taken together, our studies suggest a novel model of crosstalk between miR-487b-3p, GRM3 and TGF $\beta$  signaling (Fig. 8f). In this model, while miR-487b-3p inhibits GRM3 translation, TGF $\beta$  increases GRM3 protein stability as a negative feedback mechanism to antagonize TGF $\beta$ -induced PKA activation, AKT inhibition and suppression of cell survival, proliferation and tumorigenesis. Therefore, inhibition of GRM3 or expression of

miR-487b-3p prevents this negative feedback and enhances TGF $\beta$ -mediated tumor suppressor function.

## DISCUSSION

Although GRM3 protein expression is considerably higher in colon adenocarcinomas than in normal colon (Fig. 1), analysis of TCGA databases reveals that GRM3 mRNA remains unchanged (data not shown). It suggests that GRM3 upregulation is mediated at the posttranscriptional level. While transcriptional regulation of GRM3 has been reported (50–53), our findings that miR-487b-3p directly targets GRM3 to suppress its translation and that TGF $\beta$  increases GRM3 protein stability provide novel mechanisms of posttranscriptional regulation of GRM3 in colon cancer. Of note, GRM2, the other group II metabotropic glutamate receptor, and GRM4, reported to be present in colon cancer cells (8), are barely expressed in colon cancer cells used in the study (Fig. 2a and Fig. S5), suggesting that they may not play a role in colon cancer.

When correlating GRM3 expression with clinicopathological features of tumors, no significant correlation was found between GRM3 expression and tumor grades or stages (data not shown). However, percentage of GRM3 positive cells is noticeably higher in poorly-differentiated tumors than moderately-differentiated ones (Fig. S6a). Due to small sample size of well-differentiated tumors, the difference between well-differentiated tumors and moderately- or poor-differentiated ones is not significant. In addition, GRM3 expression is significantly higher in pancreatic tumors than in normal pancreas (Fig. S6b and S6c), indicating that upregulation of GRM3 expression is not specific to colon cancer.

It has been shown that mGluRs, such as GRM1 and mutant GRM3, activate the MEK pathway in nervous and melanoma cells (9;11). In this study, we show that GRM3 knockdown activates PKA and inhibits AKT in colon cancer cells. In addition, GRM3 knockdown or overexpression of miR-487b-3p also decreases ERK activity (Fig. S7). It indicates that GRM3 can activate multiple cancer-related signaling pathways and that the components of the glutamatergic system are active in colon cancer cells. Although we show that GRM2 expression is not upregulated in colon cancer cells, it remains to be determined whether other glutamate receptors or other elements of glutamate signaling are aberrantly expressed in colon cancer.

Our studies indicate that GRM3 antagonizes TGF $\beta$ -mediated tumor suppressor effect and that TGF $\beta$  increases GRM3 protein stability in a Smad2/3-dependent manner. These results suggest that there is a negative feedback regulation between GRM3 and TGF $\beta$  signaling (Fig. 8f). This is of significance since TGF $\beta$  is a major tumor suppressor in colon cancer (21;22;39;41). The negative feedback regulation between TGF $\beta$  and GRM3 could potentially prevent efficient intervention of tumor growth and progression by TGF $\beta$  signaling. In addition, it will be interesting to investigate whether TGF $\beta$  increases GRM3 expression in cancers where TGF $\beta$  functions as a tumor promoter (i.e. breast cancer). If so, given that GRM3 activates AKT and MEK signaling pathways, GRM3 could potentially contribute to TGF $\beta$ -mediated tumor promoting function (i.e. EMT, etc). Therefore, inhibition of GRM3 could not only enhance TGF $\beta$ -mediated tumor suppressor function but



also counteract TGF $\beta$ -mediated tumor promoting function, making targeting GRM3 an efficient anti-cancer approach despite of dual function of TGF $\beta$  signaling. Furthermore, GRM3 can also function independently of TGF $\beta$  signaling since GRM3 knockdown in HCT116 cells with defective TGF $\beta$  signaling increased apoptosis and reduced anchorage-independent growth (Fig. 2). Hence, GRM3 can be a promising molecular target in colon cancer defective of TGF $\beta$  signaling, which occurs in 30–40% of colon cancer patients.

It has been reported that GRM3 negatively regulates BMP signaling in glioma cells (12). However, we found that GRM3 knockdown did not activate BMP signaling in colon cancer cells (Fig. S8a). In addition, unlike TGF $\beta$ , BMP treatment did not increase GRM3 expression (Fig. S8b). These results suggest that BMP signaling is not likely involved in the effects mediated by GRM3 knockdown and in the regulation of GRM3 expression.

Taken together, we have identified a signaling axis, miR-487b-3p/GRM3/TGF $\beta$ /PKA/AKT, as an important regulator of tumorigenesis in colon cancer. Our studies suggest that GRM3 could be a novel molecular target for colon cancer treatment. However, one concern to target glutamate signaling for cancer treatment is whether it would affect brain or neuron function. A significant amount of work has gone into designing and testing of drugs to modulate glutamatergic system to treat neurological and psychiatric disorders. Pharmaceutical companies have generated libraries of compounds that are not optimal for treating neuropsychiatric disorders due to problems such as inability to readily penetrate blood brain barriers. However, those compounds could be ideal agents for other applications, for example, anti-cancer therapy. Since GRM3 is mainly upregulated in colon cancer but rarely expressed in normal peripheral tissues, targeting GRM3 with such agents would not likely cause adverse neurological or peripheral side effects, making GRM3 an attractive and specific target for colon cancer treatment.

## MATERIALS AND METHODS

### Cell lines and reagents

The immortalized human colon epithelial cells (HCEC) were provided by Dr. Jerry Shay (38). The human colon cancer HCT116, RKO, FET, CBS, HCT116b, GEO and HT29 cells were cultured in McCoy's 5A medium (Sigma) with 10 ng/ml epidermal growth factor (EGF), 20  $\mu$ g/ml insulin, and 4  $\mu$ g/ml transferrin (54). When subjected to GFDS, cells were cultured in medium without EGF, insulin and transferrin. Cells were maintained at 37°C in a humidified incubator with 5% CO<sub>2</sub> and checked periodically for mycoplasma contamination. TGF $\beta$ , LY341495 and miR-487b-3p inhibitor were obtained from R&D Systems, Cayman and Qiagen Inc. respectively.

### RT-PCR and Q-PCR assays

Expression of miR-487b-3p was determined by miScript primer assays and miScript SYBR® Green PCR Kit from Qiagen Inc. RNU6-2 was used as an endogenous reference gene.

Q-PCR analysis of GRM3 mRNA was performed using SYBR Green qPCR Mastermixes (Qiagen). The primer sequences are GCACCTCAACAGGTTTCAGTGT-F and TGGTGGAGTCGAGGACTTCC-R.

RT-PCR analysis of GRM2 and GRM3 mRNA was performed using primers GRM2, GAGAAGGTGGGCCGTGCCATGAG-F and CGCTGCCTGCCCGCAGATAGGT-R and GRM3, GCTCCAACATCCGCAAGTCCTA-F and TGTCATGGCCAGGTGCTTGTC-R.

### Apoptosis assays

Apoptosis was detected using a DNA fragmentation ELISA assay kit (Roche) according to manufacturer's protocol. Briefly, cells were seeded in 96-well plates and subjected to GFDS and/or treated with TGF $\beta$ . The cells were stained with MTT to determine cell numbers or lysed for ELISA assays to determine apoptosis. The relative apoptosis was determined by dividing ELISA values by MTT values of each sample.

### Soft agarose assays

Cells were seeded in medium containing low melting agar (Thermo Scientific) at 3,000 cells/well in 6-well plates. Two weeks later, colonies were stained with 1% iodinitrotetrazolium violet (Sigma-Aldrich) and counted.

### Transwell assays

Cells were seeded onto the upper surface of 8- $\mu$ m pore, 6.5 mm polycarbonate filters (Corning Costar Corp.) in medium without growth factors or serum, allowed to migrate towards medium with 10% FBS for 18 hrs and stained with MTT. The cells on the upper surface of the filter were removed with a cotton swab, and those migrated to the underside were dissolved in DMSO. Absorbance was read at 570 nm.

### Plasmids construction

The miR-487b precursor-expressing lentiviral vector, pCDH-CMV, was from SBI. ShRNAs targeting GRM3 were cloned into FSIPPW lentiviral vector. The targeting sequences of GRM3 were: sh1, 5'-CAGAACATGGAAATAACCATT-3' and sh2, 5'-GCCTGTTTCCTATTAACGAAA-3' (11). ShRNAs for Smad2 and Smad3 are 5'-GCACTTGCTCTGAAATTTG-3' and 5'-GGATTGAGCTGCACCTTGAATG-3' respectively. PKAC $\alpha$  shRNA was described previously (23). pCDF1-GRM3 was a gift from Yardena Samuels (Addgene #31798).

### Luciferase Assays

The predicted miR-487b-3p recognition site in the 3'UTR of GRM3 and corresponding mutated sequences were synthesized and cloned into psiCHECK<sup>TM</sup>-2 (Promega) downstream of Renilla reporter gene. The reporter was transfected into cells and luciferase activity was measured 48 hrs later using Dual-Luciferase Reporter Assay (Promega). Values were normalized with firefly luciferase activity.

### PKA assays

Kinase activity of PKA was measured with DetectX® PKA activity kit (Arbor assays) following manufactory's protocol.

### *In vivo* xenograft model

Animal experiments were approved by University of Nebraska Medical Center (UNMC) Institutional Animal Care and Use Committee. CBS cells ( $4 \times 10^6$ ) expressing a control vector, miR-487b precursor, a scrambled shRNA or GRM3 shRNAs were injected into the flank of 4–6 week old male athymic nude mice on both sides (Harlan Laboratories). In addition, mice injected with HCT116 cells ( $2 \times 10^6$ ) were treated with 100 mg/kg LY341495 (dissolved in 1.2 e.q. NaOH) by subcutaneous injection every day for 10 days. There were 7–8 mice and 14–16 tumors in each experimental group. Tumor volumes (V) were calculated by the formula  $V = W^2 \times L \times 0.5$ , where W represents the largest tumor diameter and L represents the next largest tumor diameter (55;56). Upon termination of the experiments, tumors were dissected out and photographed on the same scale.

### TUNEL and Ki67 staining

Formalin-fixed paraffin embedded (FFPE) tissue blocks of xenograft tumors were stained for TUNEL and Ki67 as described previously (34, 35).

### IHC staining of GRM3 in xenograft tumors and human patient samples

Human sample study was performed with the approval of Institutional Review Board. TMAs consisting of triplicates of 1 mm cores of 65 colon adenocarcinomas and 29 adjacent normal tissues of patients treated at UNMC in 2008 and 2009 were obtained from tissue core.

IHC staining was performed in paraffin slides using Novolink™ Min Polymer Detection System (Leica) as described previously (56;57). Briefly, slides were subjected to antigen retrieval using Novocastra Epitope Retrieval Solutions, pH6, followed by incubation with an anti-GRM3 antibody overnight at 4 °C. Slides were developed with DAB after incubation with Novolink polymer. Finally, slides were counterstained with hematoxylin. For each sample, ten randomly chosen fields were captured at 40 × magnification and quantified with Imagescope Software (Aperio Technologies, Inc.).

### In Situ hybridization

The double DIG labeled probe for miR487b-3p and hybridization kit were purchased from Exiqon. Hybridization was performed following Exiqon's protocol. Briefly, tissues were deparaffinized and digested with proteinase K (15 µg/ml; Exiqon) for 10 min at 37°C. Slides were incubated in hybridization buffer with 40 nM miR-487b-3p probe (5DigN/AAGTGGATGACCCTGTACGATT/3Dig\_N/) in a humidified chamber at 45°C overnight. Slides were then blocked with anti-digoxigenin-alkaline phosphatase antibodies (Roche) at 1:800 dilution for 1 hr and stained with AP substrate (NBT/BCIP tablet, Roche) at 30°C for 6 hrs. The nuclei were counterstained with nuclear fast red (Sigma). The staining intensity was determined using image pro plus (Media Cybernetics, Inc.).

## Statistical analysis

Statistical analyses were performed using Bonferroni two-sided t-test, two-way ANOVA or Student's t-test.

## Supplementary Material

Refer to Web version on PubMed Central for supplementary material.

## Acknowledgments

This work was supported by NIH/NCI R01CA140988-01 to J.W. H.Y. was partially supported by Chinese Scholar Council.

## References

1. Curtis DR, Phillis JW, Watkins JC. Chemical excitation of spinal neurones. *Nature*. 1959; 183:611–612. [PubMed: 13632811]
2. Hayashi T. A physiological study of epileptic seizures following cortical stimulation in animals and its application to human clinics. *Jpn J Physiol*. 1952; 3:46–64. [PubMed: 13034377]
3. Tanabe Y, Masu M, Ishii T, Shigemoto R, Nakanishi S. A family of metabotropic glutamate receptors. *Neuron*. 1992; 8:169–179. [PubMed: 1309649]
4. Aramori I, Nakanishi S. Signal transduction and pharmacological characteristics of a metabotropic glutamate receptor, mGluR1, in transfected CHO cells. *Neuron*. 1992; 8:757–765. [PubMed: 1314623]
5. Skerry TM, Genever PG. Glutamate signalling in non-neuronal tissues. *Trends Pharmacol Sci*. 2001; 22:174–181. [PubMed: 11282417]
6. Hoogduijn MJ, Hitchcock IS, Smit NP, Gillbro JM, Schallreuter KU, Genever PG. Glutamate receptors on human melanocytes regulate the expression of MiTF. *Pigment Cell Res*. 2006; 19:58–67. [PubMed: 16420247]
7. Tong Q, Ouedraogo R, Kirchgessner AL. Localization and function of group III metabotropic glutamate receptors in rat pancreatic islets. *Am J Physiol Endocrinol Metab*. 2002; 282:E1324–E1333. [PubMed: 12006363]
8. Chang HJ, Yoo BC, Lim SB, Jeong SY, Kim WH, Park JG. Metabotropic glutamate receptor 4 expression in colorectal carcinoma and its prognostic significance. *Clin Cancer Res*. 2005; 11:3288–3295. [PubMed: 15867225]
9. Martino JJ, Wall BA, Mastrantoni E, Wilimczyk BJ, La Cava SN, Degenhardt K, et al. Metabotropic glutamate receptor 1 (Grm1) is an oncogene in epithelial cells. *Oncogene*. 2013; 32:4366–4376. [PubMed: 23085756]
10. Kim MS, Chang X, Nagpal JK, Yamashita K, Baek JH, Dasgupta S, et al. The N-methyl-D-aspartate receptor type 2A is frequently methylated in human colorectal carcinoma and suppresses cell growth. *Oncogene*. 2008; 27:2045–2054. [PubMed: 17922030]
11. Prickett TD, Wei X, Cardenas-Navia I, Teer JK, Lin JC, Walia V, et al. Exon capture analysis of G protein-coupled receptors identifies activating mutations in GRM3 in melanoma. *Nat Genet*. 2011; 43:1119–1126. [PubMed: 21946352]
12. Ciceroni C, Arcella A, Mosillo P, Battaglia G, Mastrantoni E, Oliva MA, et al. Type-3 metabotropic glutamate receptors negatively modulate bone morphogenetic protein receptor signaling and support the tumorigenic potential of glioma-initiating cells. *Neuropharmacology*. 2008; 55:568–576. [PubMed: 18621067]
13. Arcella A, Carpinelli G, Battaglia G, D'Onofrio M, Santoro F, Ngomba RT, et al. Pharmacological blockade of group II metabotropic glutamate receptors reduces the growth of glioma cells in vivo. *Neuro Oncol*. 2005; 7:236–245. [PubMed: 16053698]

14. D'Onofrio M, Arcella A, Bruno V, Ngomba RT, Battaglia G, Lombardi V, et al. Pharmacological blockade of mGlu2/3 metabotropic glutamate receptors reduces cell proliferation in cultured human glioma cells. *J Neurochem.* 2003; 84:1288–1295. [PubMed: 12614329]
15. Zhou K, Song Y, Zhou W, Zhang C, Shu H, Yang H, et al. mGlu3 receptor blockade inhibits proliferation and promotes astrocytic phenotype in glioma stem cells. *Cell Biol Int.* 2014; 38:426–434. [PubMed: 24482010]
16. Wakefield LM, Roberts AB. TGF-beta signaling: positive and negative effects on tumorigenesis. *Curr Opin Genet Dev.* 2002; 12:22–29. [PubMed: 11790550]
17. Bu P, Wang L, Chen KY, Rakhilin N, Sun J, Closa A, et al. miR-1269 promotes metastasis and forms a positive feedback loop with TGF-beta. *Nat Commun.* 2015; 6:6879. [PubMed: 25872451]
18. Calon A, Espinet E, Palomo-Ponce S, Tauriello DV, Iglesias M, Cespedes MV, et al. Dependency of colorectal cancer on a TGF-beta-driven program in stromal cells for metastasis initiation. *Cancer Cell.* 2012; 22:571–584. [PubMed: 23153532]
19. Gulubova M, Manolova I, Ananiev J, Julianov A, Yovchev Y, Peeva K. Role of TGF-beta1, its receptor TGFbetaRII, and Smad proteins in the progression of colorectal cancer. *Int J Colorectal Dis.* 2010; 25:591–599. [PubMed: 20165854]
20. Wang J, Yang L, Yang J, Kuropatwinski K, Wang W, Liu XQ, et al. Transforming growth factor beta induces apoptosis through repressing the phosphoinositide 3-kinase/AKT/survivin pathway in colon cancer cells. *Cancer Res.* 2008; 68:3152–3160. [PubMed: 18451140]
21. Wang J, Sun L, Myeroff L, Wang X, Gentry LE, Yang J, et al. Demonstration that mutation of the type II transforming growth factor beta receptor inactivates its tumor suppressor activity in replication error-positive colon carcinoma cells. *J Biol Chem.* 1995; 270:22044–22049. [PubMed: 7665626]
22. Wang J, Han W, Zborowska E, Liang J, Wang X, Willson JK, et al. Reduced expression of transforming growth factor beta type I receptor contributes to the malignancy of human colon carcinoma cells. *J Biol Chem.* 1996; 271:17366–17371. [PubMed: 8663343]
23. Chowdhury S, Howell GM, Rajput A, Teggart CA, Brattain LE, Weber HR, et al. Identification of a novel TGFbeta/PKA signaling transduceome in mediating control of cell survival and metastasis in colon cancer. *PLoS ONE.* 2011; 6:e19335. [PubMed: 21559296]
24. Simms N, Rajput A, Sharratt EA, Ongchin M, Teggart CA, Wang J, et al. Transforming growth factor-ss suppresses metastasis in a subset of human colon carcinoma cells. *BMC Cancer.* 2012; 12:221. [PubMed: 22672900]
25. Forrester E, Chytil A, Bierie B, Aakre M, Gorska AE, Sharif-Afshar AR, et al. Effect of conditional knockout of the type II TGF-beta receptor gene in mammary epithelia on mammary gland development and polyomavirus middle T antigen induced tumor formation and metastasis. *Cancer Res.* 2005; 65:2296–2302. [PubMed: 15781643]
26. Yang L, Huang J, Ren X, Gorska AE, Chytil A, Aakre M, et al. Abrogation of TGF beta signaling in mammary carcinomas recruits Gr-1+CD11b+ myeloid cells that promote metastasis. *Cancer Cell.* 2008; 13:23–35. [PubMed: 18167337]
27. Veenendaal LM, Kranenburg O, Smakman N, Klomp A, Borel RI, van Diest PJ. Differential Notch and TGFbeta signaling in primary colorectal tumors and their corresponding metastases. *Cell Oncol.* 2008; 30:1–11. [PubMed: 18219106]
28. Bacman D, Merkel S, Croner R, Papadopoulos T, Brueckl W, Dimmler A. TGF-beta receptor 2 downregulation in tumour-associated stroma worsens prognosis and high-grade tumours show more tumour-associated macrophages and lower TGF-beta1 expression in colon carcinoma: a retrospective study. *BMC Cancer.* 2007; 7:156. [PubMed: 17692120]
29. Hamamoto T, Beppu H, Okada H, Kawabata M, Kitamura T, Miyazono K, et al. Compound disruption of smad2 accelerates malignant progression of intestinal tumors in apc knockout mice. *Cancer Res.* 2002; 62:5955–5961.
30. Munoz NM, Upton M, Rojas A, Washington MK, Lin L, Chytil A, et al. Transforming growth factor beta receptor type II inactivation induces the malignant transformation of intestinal neoplasms initiated by Apc mutation. *Cancer Res.* 2006; 66:9837–9844. [PubMed: 17047044]

31. Sodir NM, Chen X, Park R, Nickel AE, Conti PS, Moats R, et al. Smad3 deficiency promotes tumorigenesis in the distal colon of ApcMin/+ mice. *Cancer Res.* 2006; 66:8430–8438. [PubMed: 16951153]
32. Takaku K, Oshima M, Miyoshi H, Matsui M, Seldin MF, Taketo MM. Intestinal tumorigenesis in compound mutant mice of both Dpc4 (Smad4) and Apc genes. *Cell.* 1998; 92:645–656. [PubMed: 9506519]
33. Zeng Q, Phukan S, Xu Y, Sadim M, Rosman DS, Pennison M, et al. Tgfbr1 haploinsufficiency is a potent modifier of colorectal cancer development. *Cancer Res.* 2009; 69:678–686. [PubMed: 19147584]
34. Du T, Zamore PD. microPrimer: the biogenesis and function of microRNA. *Development.* 2005; 132:4645–4652. [PubMed: 16224044]
35. Bartel DP. MicroRNAs: target recognition and regulatory functions. *Cell.* 2009; 136:215–233. [PubMed: 19167326]
36. Zhang B, Pan X, Cobb GP, Anderson TA. microRNAs as oncogenes and tumor suppressors. *Dev Biol.* 2007; 302:1–12. [PubMed: 16989803]
37. Schoepp DD, Jane DE, Monn JA. Pharmacological agents acting at subtypes of metabotropic glutamate receptors. *Neuropharmacology.* 1999; 38:1431–1476. [PubMed: 10530808]
38. Roig AI, Eskiocak U, Hight SK, Kim SB, Delgado O, Souza RF, et al. Immortalized epithelial cells derived from human colon biopsies express stem cell markers and differentiate in vitro. *Gastroenterology.* 2010; 138:1012–1021. [PubMed: 19962984]
39. Markowitz S, Wang J, Myeroff L, Parsons R, Sun L, Lutterbaugh J, et al. Inactivation of the type II TGF-beta receptor in colon cancer cells with microsatellite instability. *Science.* 1995; 268:1336–1338. [PubMed: 7761852]
40. Chowdhury S, Ongchin M, Sharratt E, Dominguez I, Wang J, Brattain MG, et al. Intra-tumoral heterogeneity in metastatic potential and survival signaling between iso-clonal HCT116 and HCT116b human colon carcinoma cell lines. *PLoS ONE.* 2013; 8:e60299. [PubMed: 23560089]
41. Ye SC, Foster JM, Li W, Liang J, Zborowska E, Venkateswarlu S, et al. Contextual effects of transforming growth factor beta on the tumorigenicity of human colon carcinoma cells. *Cancer Res.* 1999; 59:4725–4731. [PubMed: 10493532]
42. Woodford-Richens KL, Rowan AJ, Gorman P, Halford S, Bicknell DC, Wasan HS, et al. SMAD4 mutations in colorectal cancer probably occur before chromosomal instability, but after divergence of the microsatellite instability pathway. *Proc Natl Acad Sci U S A.* 2001; 98:9719–9723. [PubMed: 11481457]
43. da Costa LT, He TC, Yu J, Sparks AB, Morin PJ, Polyak K, et al. CDX2 is mutated in a colorectal cancer with normal APC/beta-catenin signaling. *Oncogene.* 1999; 18:5010–5014. [PubMed: 10490837]
44. Kingston AE, Ornstein PL, Wright RA, Johnson BG, Mayne NG, Burnett JP, et al. LY341495 is a nanomolar potent and selective antagonist of group II metabotropic glutamate receptors. *Neuropharmacology.* 1998; 37:1–12. [PubMed: 9680254]
45. Banerjee A, Pirrone V, Wigdahl B, Nonnemacher MR. Transcriptional regulation of the chemokine co-receptor CCR5 by the cAMP/PKA/CREB pathway. *Biomed Pharmacother.* 2011; 65:293–297. [PubMed: 21719243]
46. Geng L, Chaudhuri A, Talmon G, Wisecarver JL, Wang J. TGF-Beta suppresses VEGFA-mediated angiogenesis in colon cancer metastasis. *PLoS ONE.* 2013; 8:e59918. [PubMed: 23536895]
47. Grimson A, Farh KK, Johnston WK, Garrett-Engel P, Lim LP, Bartel DP. MicroRNA targeting specificity in mammals: determinants beyond seed pairing. *Mol Cell.* 2007; 27:91–105. [PubMed: 17612493]
48. Krek A, Grun D, Poy MN, Wolf R, Rosenberg L, Epstein EJ, et al. Combinatorial microRNA target predictions. *Nat Genet.* 2005; 37:495–500. [PubMed: 15806104]
49. Betel D, Koppal A, Agius P, Sander C, Leslie C. Comprehensive modeling of microRNA targets predicts functional non-conserved and non-canonical sites. *Genome Biol.* 2010; 11:R90. [PubMed: 20799968]

50. Cha JH, Kosinski CM, Kerner JA, Alsdorf SA, Mangiarini L, Davies SW, et al. Altered brain neurotransmitter receptors in transgenic mice expressing a portion of an abnormal human huntington disease gene. *Proc Natl Acad Sci U S A*. 1998; 95:6480–6485. [PubMed: 9600992]
51. Lourenco NF, Schadrack J, Platzer S, Zieglgansberger W, Tolle TR, Castro-Lopes JM. Expression of metabotropic glutamate receptors mRNA in the thalamus and brainstem of monoarthritic rats. *Brain Res Mol Brain Res*. 2000; 81(1–2):140–154. [PubMed: 11000486]
52. Minoshima T, Nakanishi S. Structural organization of the mouse metabotropic glutamate receptor subtype 3 gene and its regulation by growth factors in cultured cortical astrocytes. *J Biochem*. 1999; 126:889–896. [PubMed: 10544282]
53. Neto FL, Schadrack J, Platzer S, Zieglgansberger W, Tolle TR, Castro-Lopes JM. Up-regulation of metabotropic glutamate receptor 3 mRNA expression in the cerebral cortex of monoarthritic rats. *J Neurosci Res*. 2001; 63:356–367. [PubMed: 11170186]
54. Boyd DD, Levine AE, Brattain DE, McKnight MK, Brattain MG. Comparison of growth requirements of two human intratumoral colon carcinoma cell lines in monolayer and soft agarose. *Cancer Res*. 1988; 48:2469–2474. [PubMed: 3281751]
55. Zhang Y, Geng L, Talmon G, Wang J. MicroRNA-520g confers drug resistance by regulating p21 expression in colorectal cancer. *J Biol Chem*. 2015; 290:6215–6225. [PubMed: 25616665]
56. Zhang Y, Talmon G, Wang J. MicroRNA-587 antagonizes 5-FU-induced apoptosis and confers drug resistance by regulating PPP2R1B expression in colorectal cancer. *Cell Death Dis*. 2015; 6:e1845. [PubMed: 26247730]
57. Geng L, Chaudhuri A, Talmon G, Wisecarver JL, Are C, Brattain M, et al. MicroRNA-192 suppresses liver metastasis of colon cancer. *Oncogene*. 2014; 33:5332–5340. [PubMed: 24213572]

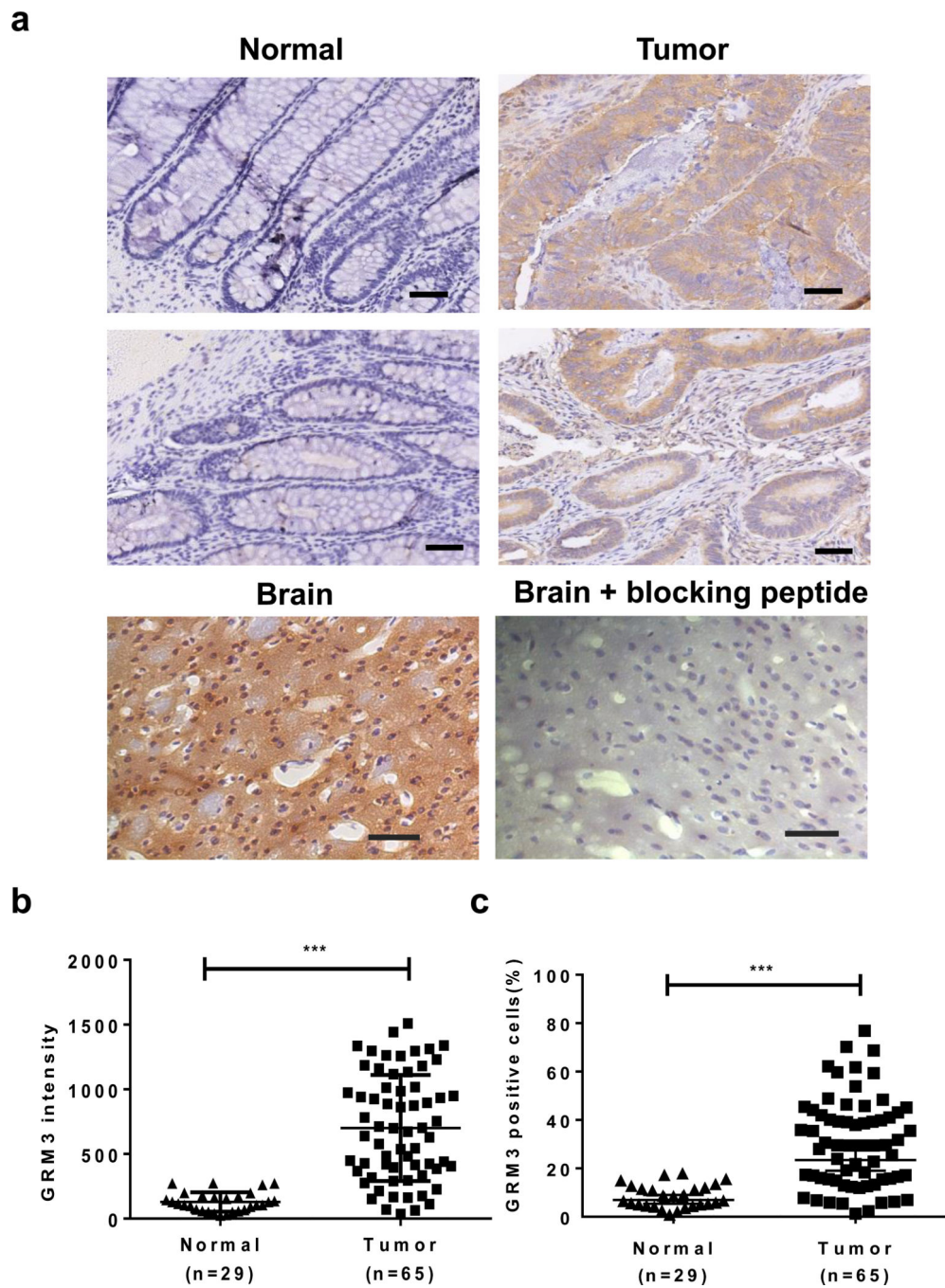


**Figure 1. GRM3 expression is elevated significantly in colon cancer specimens**

**a**, Immunohistochemistry staining of GRM3 was performed in normal colon and colon adenocarcinomas. Mouse brain tissue stained with the anti-GRM3 antibody in the absence or presence of a specific blocking peptide was used as a positive and negative control respectively. Representative images are shown. Scale bars, 100  $\mu$ m. **b&c**, Quantification of GRM3 staining intensity (**b**) and percentage of GRM3 positive cells (**c**) was performed. The values of individual samples are shown. Error bars indicate SEM of the values. \*\*\*  $P < 0.001$ .



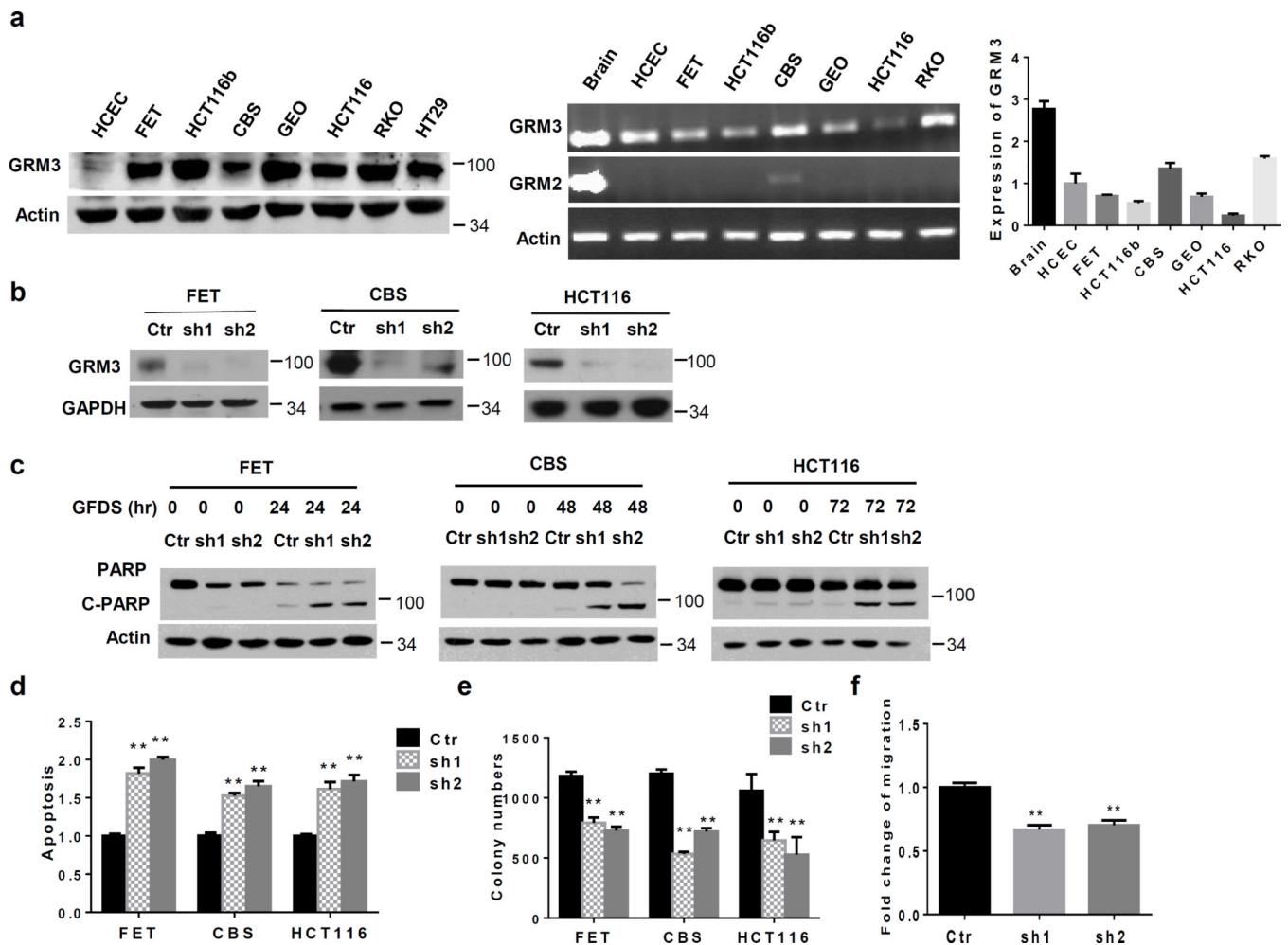


**Figure 2. GRM3 expression is upregulated in colon cancer cells**

**a**, GRM3 expression was determined in colon cancer cell lines and HCECs by western blot analysis (left). GRM2 and GRM3 mRNA expression was determined by RT-PCR assays. Mouse brain tissue was used as a positive control (middle). GRM3 mRNA expression was determined by Q-PCR assays (right). **b**, GRM3 expression was knocked down by two shRNAs. **c&d**, Control or GRM3 knockdown cells were subjected to GFDS. Cleaved PARP (**c**) and apoptosis (**d**) were determined. **e**, Colony numbers were determined in soft agarose assays of control or GRM3 knockdown cells. **f**, Cell motility and migration were determined in Transwell assays of control or GRM3 knockdown HCT116 cells. The data are presented as the mean  $\pm$  SD of three replications. \*\*  $P < 0.01$ .

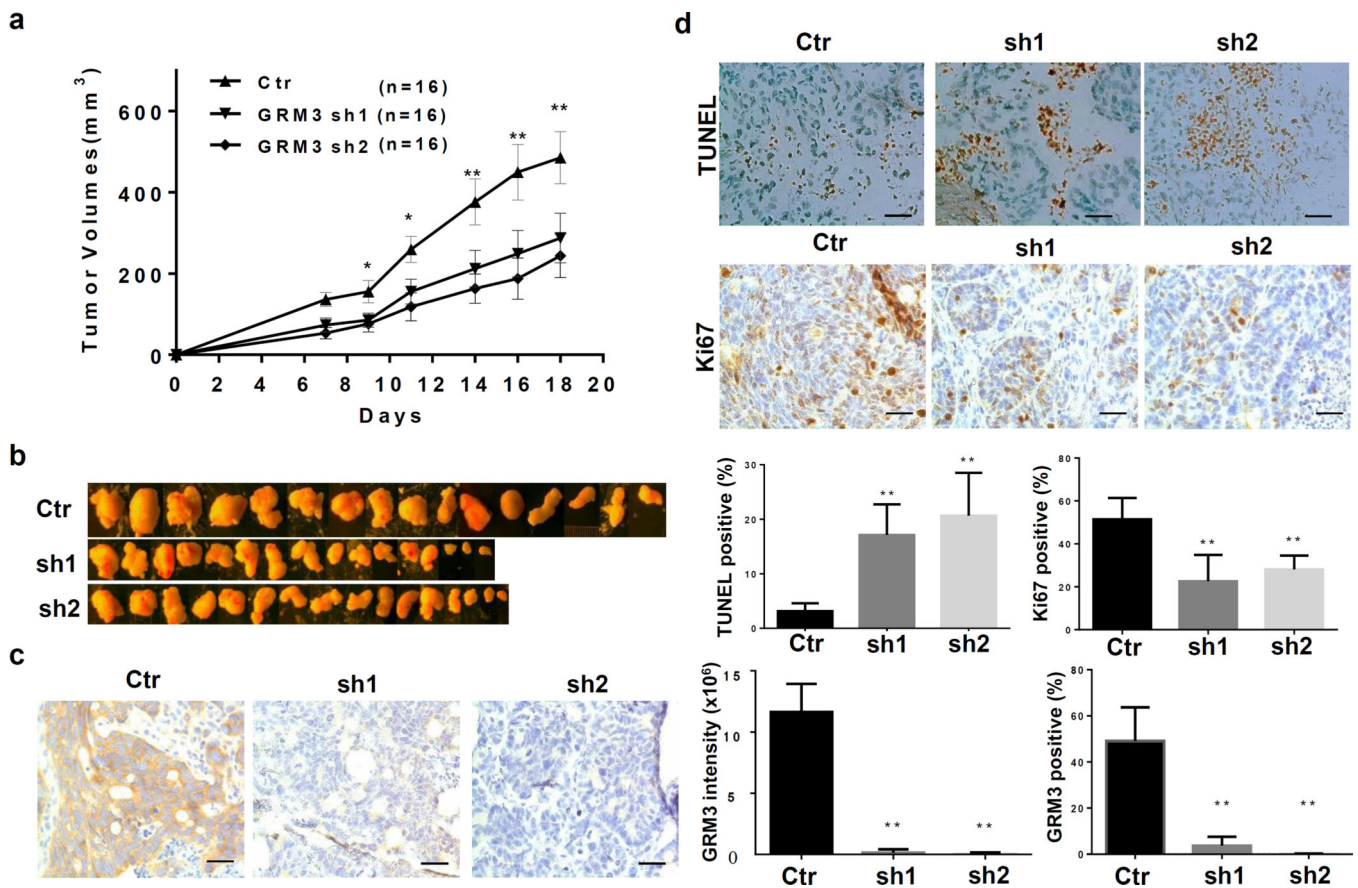


**Figure 3. GRM3 mediates tumor growth *in vivo***

**a**, Xenograft tumor growth curves of CBS control and GRM3 shRNA-expressing cells are shown.  $n=16$ . **b**, Images of tumors at the endpoint of experiments are shown. The pictures were taken on the same scale with the ruler with each tumor (Fig. S9). **c**, Representative images of GRM3 staining in xenograft tumors are shown (left). Quantification of staining intensity and percentage of GRM3 positive cells was performed (right). **d**, Representative images of TUNEL and Ki67 staining are shown (upper). Percentage of positive staining cells was determined (lower). Scale bars, 100  $\mu\text{m}$ . The data are presented as the mean  $\pm$  SD. \* $P < 0.05$ , \*\*  $P < 0.01$ .

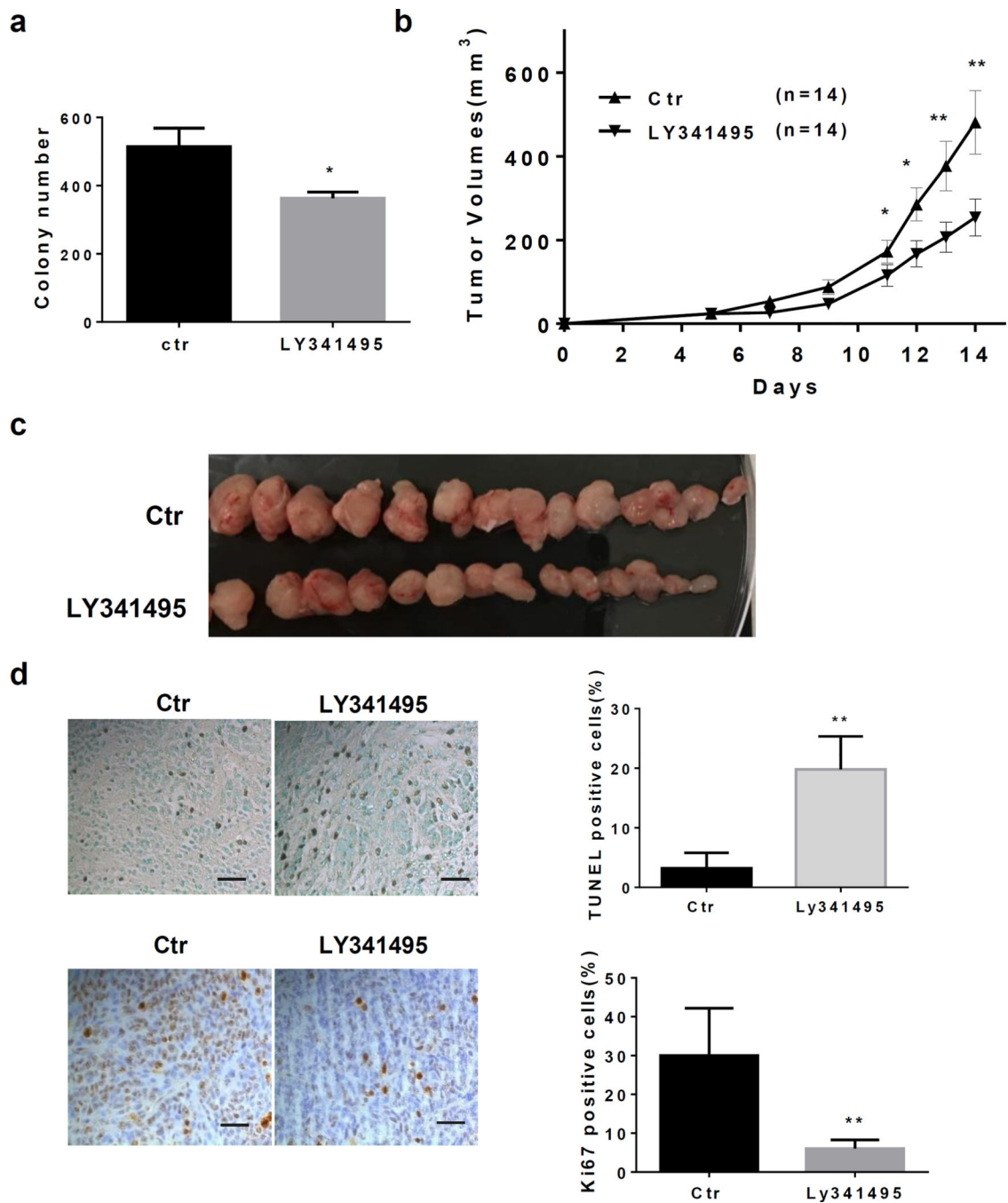


**Figure 4. The GRM3 antagonist inhibits tumor growth *in vivo***

**a**, Colony numbers were determined in soft agarose assays of control or LY341495-treated HCT116 cells. **b**, Xenograft tumor growth curves of HCT116 cells treated with LY341495 or vehicle are shown.  $n=14$ . **c**, Images of tumors at the endpoint of experiments are shown. **d**, Representative images of TUNEL and Ki67 staining are shown (left). Percentage of positive staining cells was determined (right). Scale bars, 100  $\mu\text{m}$ . The data are presented as the mean  $\pm$  SD. \* $P < 0.05$ , \*\* $P < 0.01$ .

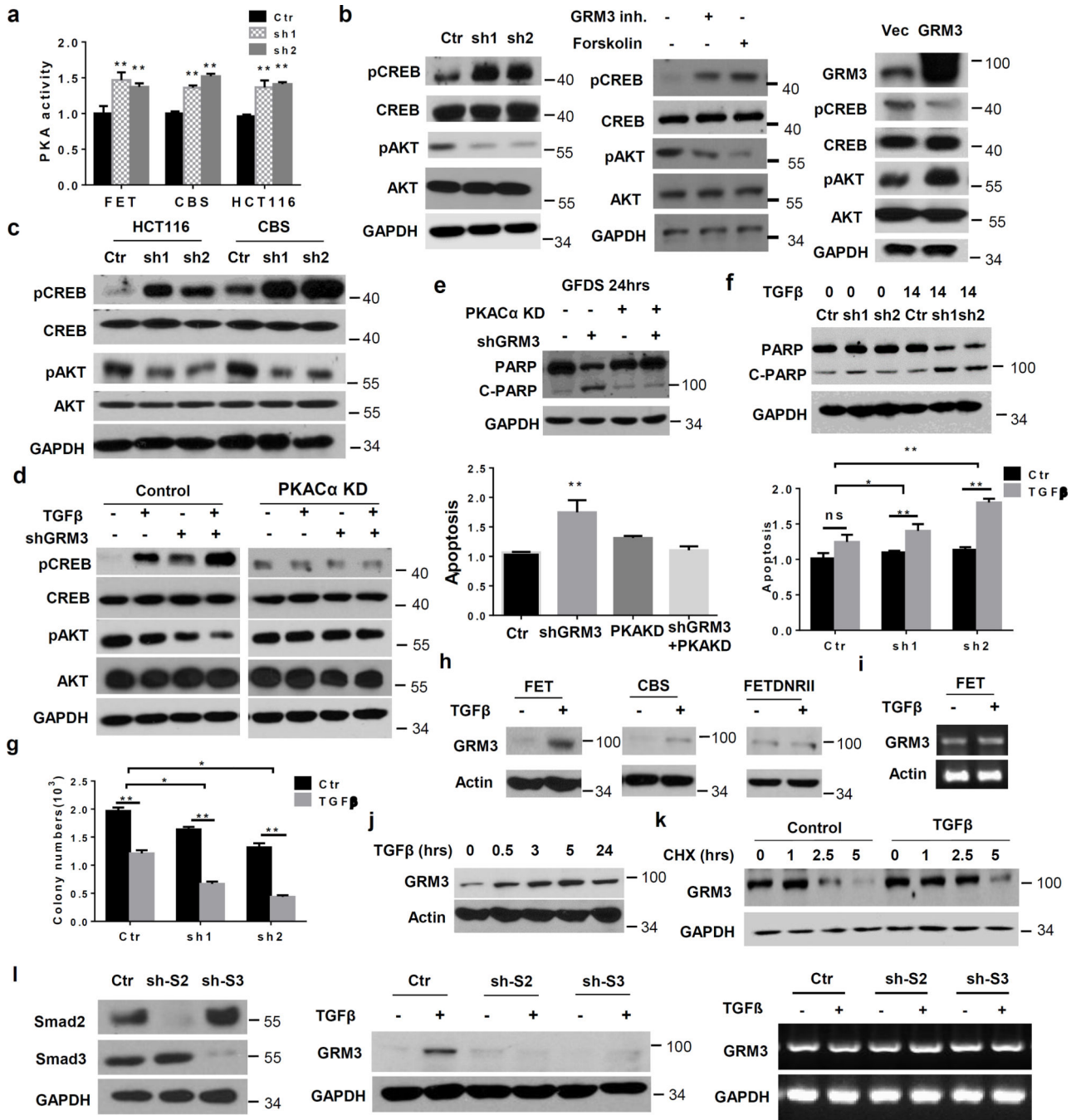


**Figure 5. GRM3 antagonizes TGFβ-mediated activation of PKA/AKT**

**a**, PKA activity was determined in FET, HCT116 and CBS cells. **b**, pCREB, and pAKT were determined in FET control and GRM3 knockdown cells (left), FET cells treated with LY341495 or forskolin (middle) and vector- or GRM3-expressing FET cells (right). **c&d**, pCREB, and pAKT were determined in HCT116 and CBS control and GRM3 knockdown cells (**c**) and FET control and PKACα. KD cells each infected with GRM3 sh2 or treated with 4 ng/ml TGFβ or both (**d**). **e**, PKACα was knocked down in FET control or GRM3 knockdown cells. Cells were subjected to GFDS for 24 hrs. Cleaved PARP (upper) and

apoptosis (lower) were determined. **f**, FET control or GRM3 knockdown cells were treated with 4 ng/ml TGF $\beta$  under GFDS for 14 hrs. Cleaved PARP (upper) and apoptosis (lower) were determined. **g**, Colony numbers were determined in soft agarose assays of FET control or GRM3 knockdown cells treated with 0.5 ng/ml TGF $\beta$ . **h**, Cells were treated with 4 ng/ml TGF $\beta$  for 6 hrs. GRM3 expression was determined by western blot assays. **i**, FET cells were treated with 4 ng/ml TGF $\beta$  for 6 hrs. GRM3 mRNA was determined by RT-PCR assays. **j**, FET cells were treated with 4 ng/ml TGF $\beta$  for the indicated time. GRM3 expression was determined by western blot assays. **k**, FET cells were treated with cycloheximide in the presence or absence of TGF $\beta$ . GRM3 expression was determined by western blot assays. **l**, Expression of Smad2 or Smad3 was knocked down individually in FET cells (left). Cells were treated with TGF $\beta$ . GRM3 protein and mRNA expression was determined by western blot assays (middle) and RT-PCR analysis (right) respectively. The data are presented as the mean  $\pm$  SD of three replications. \*  $P < 0.05$ , \*\*  $P < 0.01$ .

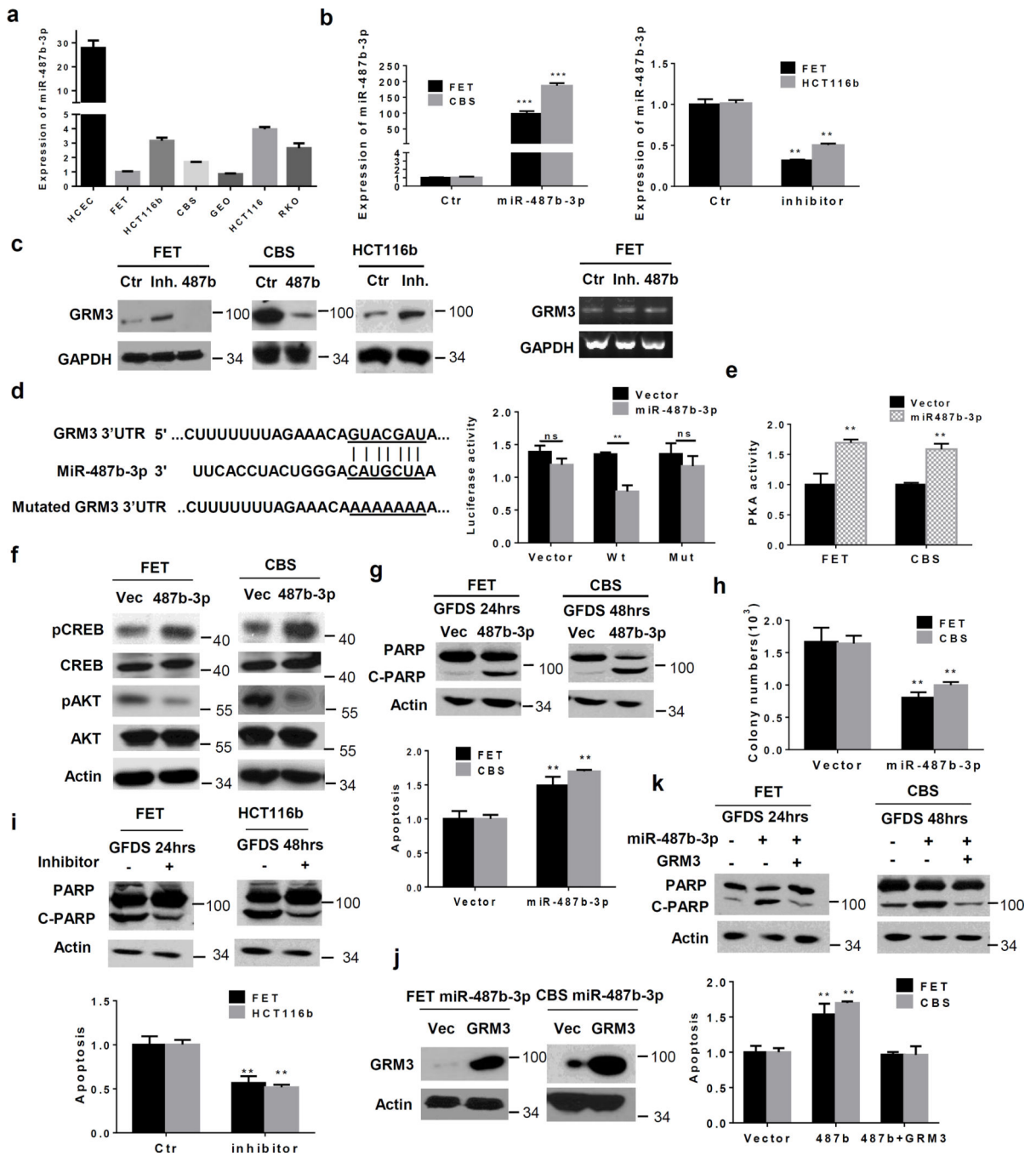


**Figure 6. GRM3 is a direct target of miR-487b-3p**

**a**, Expression of miR-487b-3p was determined in HCECs and colon cancer cells by Q-PCR assays. **b**, Expression of miR-487b-3p was determined after infection with miR-487b precursor (left) or transfection with the miR-487b inhibitor (right). **c**, GRM3 expression was determined by western blot assays (left) and by RT-PCR assays (right) after infected with miR-487b precursor or transfected with the miR-487b-3p inhibitor. **d**, The predicted miR-487b-3p recognition site in the 3'UTR of GRM3 and corresponding mutated sequences are indicated by lines (left). After transfection with psiCheck-2 constructs containing the

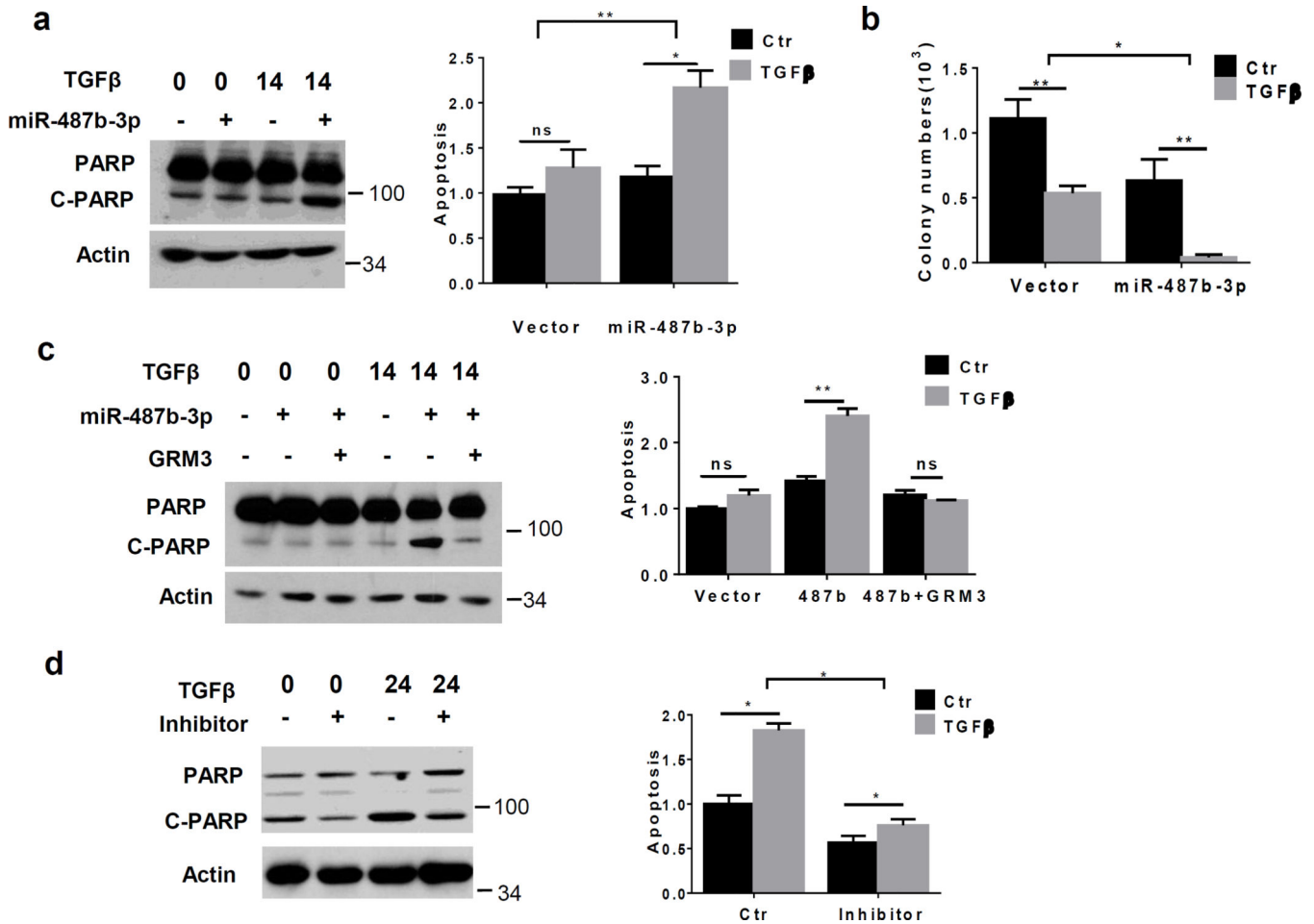
wild type (Wt) or mutant (Mut) sequences, luciferase assays were performed in FET control and miR-487b-3p expressing cells (right). **e**, PKA activity was determined in colon cancer cells. **f**, pCREB and pAKT were determined in vector- or miR-487b-3p-expressing FET and CBS cells. **g**, Vector- or miR-487b-3p-expressing FET and CBS cells were subject to GFDS for 24 and 48 hrs respectively. Cleaved PARP (upper) and apoptosis (lower) were determined. **h**, Colony numbers were determined in soft agarose assays of vector- or miR-487b-3p-expressing FET and CBS cells. **i**, FET and HCT116b cells transfected with the miR-487b-3p inhibitor were subjected to GFDS for 24 or 48 hrs respectively. Cleaved PARP (upper) and apoptosis (lower) were determined. **j&k**, GRM3 was ectopically expressed in miR-487b-3p-expressing FET and CBS cells (**j**), which were subjected to GFDS for 24 and 48 hrs respectively. Cleaved PARP (**k**, upper) and apoptosis (**k**, lower) were determined. The data are presented as the mean  $\pm$  SD of three replications. \*\*  $P < 0.01$ , \*\*\*  $P < 0.001$ .

Author Manuscript

Author Manuscript

Author Manuscript

Author Manuscript





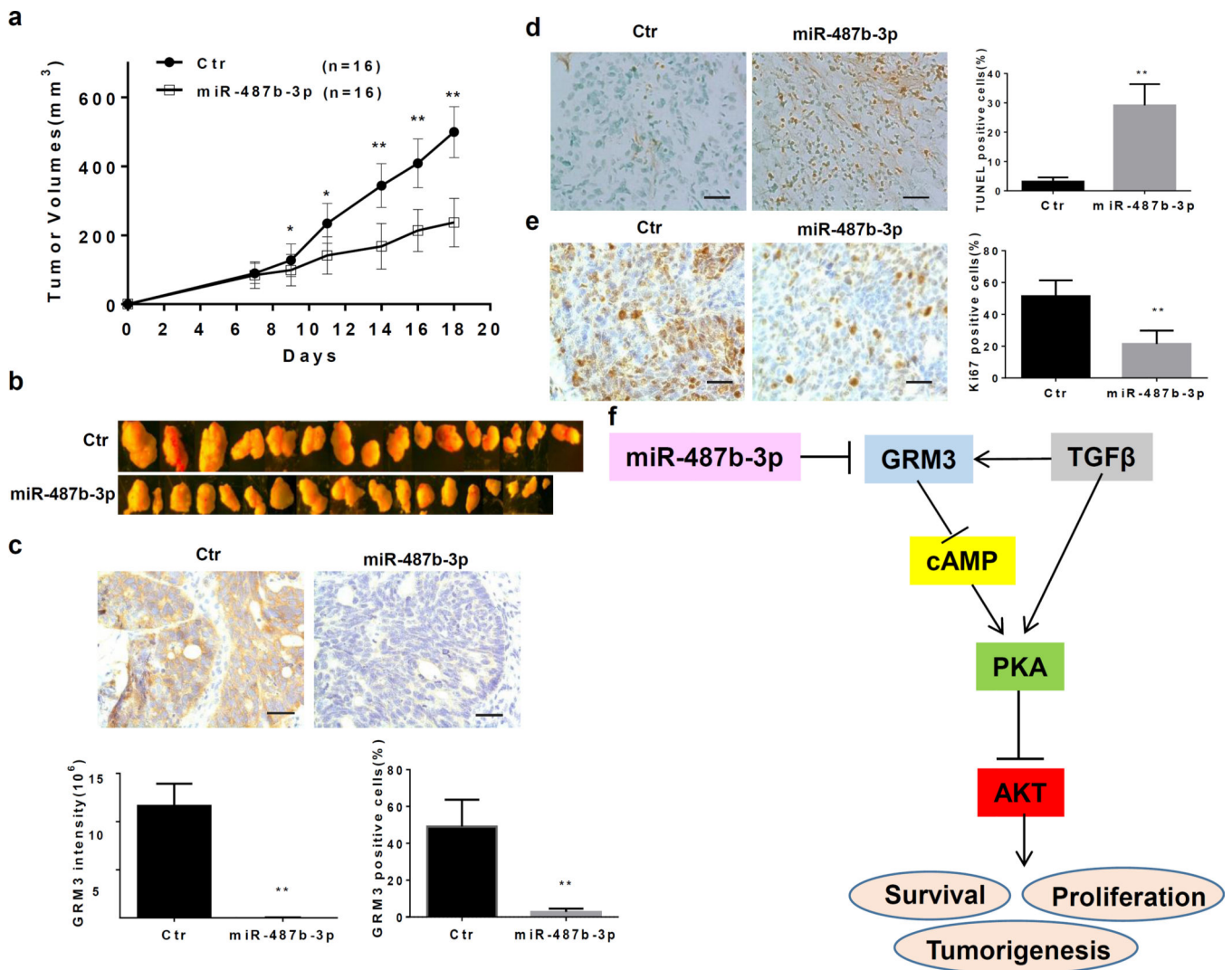


**Figure 8. MiR-487b-3p suppresses GRM3 expression and inhibits tumor growth *in vivo***

**a.** Xenograft tumor growth curves of CBS control and miR-487b-3p-expressing cells is shown. n=16. **b.** Representative images of tumors at the endpoint of experiments are shown. The pictures were taken on the same scale with the ruler with each tumor (Fig. S10). **c.** Representative images of GRM3 staining in xenograft tumors are shown (upper). Quantification of staining intensity and percentage of GRM3 positive cells was performed (lower). **d&e.** Representative images of TUNEL (**d**) and Ki67 (**e**) staining are shown (left). Percentage of positive TUNEL (**d**) and Ki67 (**e**) staining cells were determined (right). Scale bars, 100  $\mu$ m. The data are presented as the mean  $\pm$  SD. \* $P < 0.05$ , \*\* $P < 0.01$ . **f.** A proposed model of crosstalk between miR-487b-3p, GRM3 and TGF $\beta$  signaling in regulation of PKA/AKT activation, cell survival, proliferation and tumorigenesis of colon cancer cells.

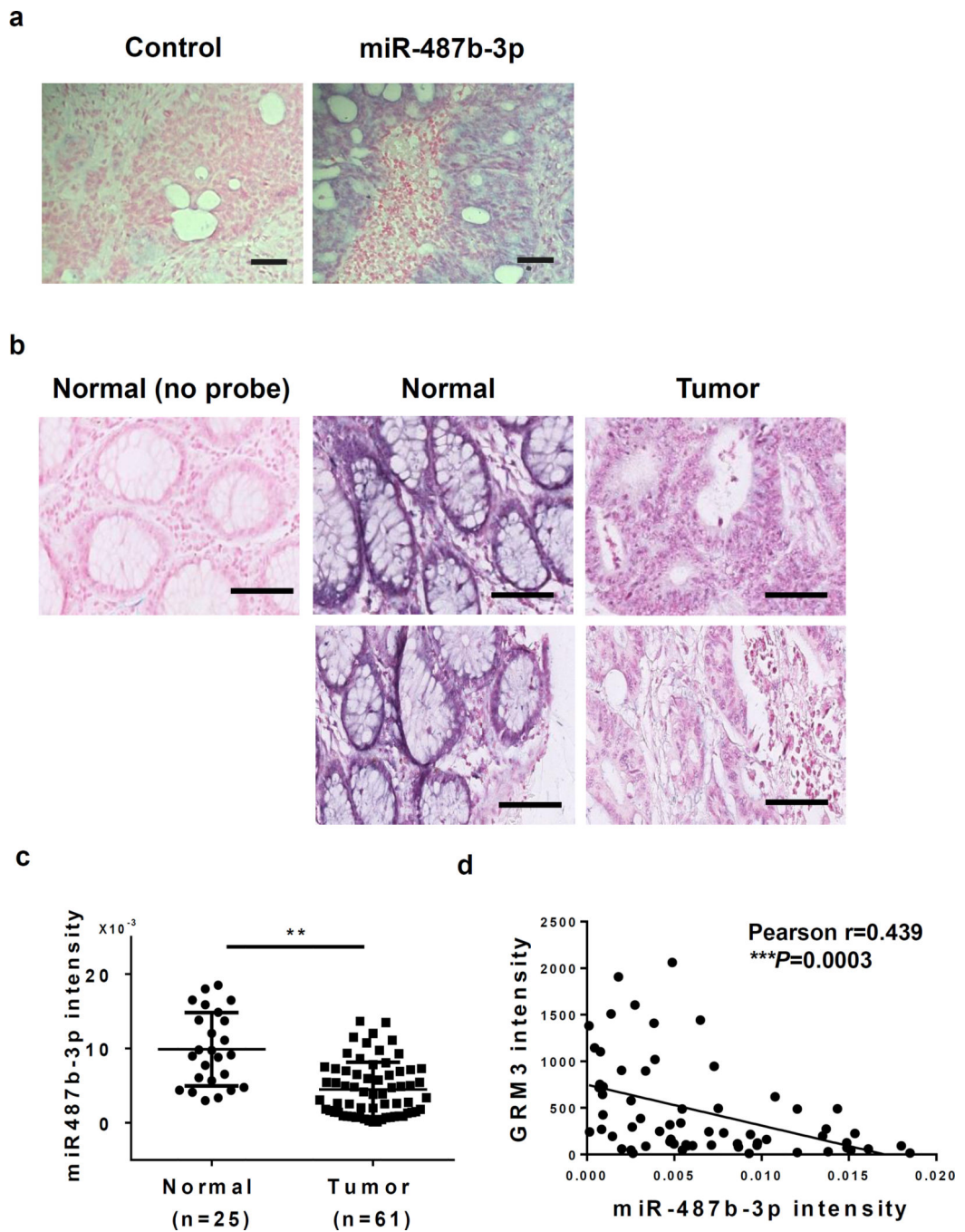


**Figure 9. Expression of miR-487b-3p is decreased in colon cancer specimens**

*In situ* hybridization analysis of miR-487b-3p was performed in xenograft tumors and human specimens. **a**, Representative images of miR-487b-3p staining in xenograft tumors are shown. Scale bars, 100  $\mu\text{m}$ . **b**, Normal colon in the absence of the probe was used as a negative control. Representative images of miR-487b-3p staining in normal colon and colon tumors are shown. Scale bars, 100  $\mu\text{m}$ . **c**, Quantification of the staining intensity was performed. The values of individual samples are shown. Error bars indicate SEM of the values. \*\*  $P < 0.01$ . **d**, Correlation of expression of miR-487b-3p and GRM3 was

determined using Pearson's test ( $r = 0.439$ , \*\*\*  $P = 0.0003$ ;  $n = 64$ ). The slope was generated by lineage regression analysis.

Author Manuscript

Author Manuscript

Author Manuscript

Author Manuscript